Regenerative Engineering and Translational Medicine (2019) 5:362–372
https://doi.org/10.1007/s40883-019-00092-8

Production and Characterization of Recombinant Collagen-Binding Resilin Nanocomposite for Regenerative Medicine Applications

Paiyz E. Mikael[1] · Ranodhi Udangawa[1,2] · Mirco Sorci[1] · Brady Cress[1,3] · Zvi Shtein[4,5] · Georges Belfort[1,3] · Oded Shoseyov[4,5] · Jonathan S. Dordick[1,3] · Robert J. Linhardt[1,2,3]

Received: 6 December 2018 / Accepted: 28 January 2019 / Published online: 19 February 2019

Abstract

Development of mechanically stable and multifunctional biomaterials for sensing, repair, and regeneration applications is of great importance. Herein, we investigate the potential of recombinant resilin-like (Res) nanocomposite elastomer as a template biomaterial for regenerative devices such as adhesive bandages or films, electrospun fibers, screws, sutures, and drug delivery vehicles. Exon I (Rec1) from the native resilin gene of *Drosophila* (CG15920) was fused with collagen-binding domain (ColBD) from *Clostridium histolyticum* and expressed in *Komagataella pastoris* (formerly *Pichia pastoris*). The 100% binding of Resilin-ColBD (Res-ColBD) to collagen I was shown at a 1:1 ratio by mass. Atomic force microscopy results in force mode show a bimodal profile for the ColBD-binding interactions. Moreover, based on the force-volume map, Res-ColBD adhesion to collagen was statistically significantly higher than resilin without ColBD.

Lay Summary

Designing advanced biomaterials that will not only withstand the repetitive mechanical loading and flexibility of tissues but also retain biochemical and biophysical interactions remains challenging. The combination of physical, biological, and chemical cues is vital for disease regulation, healing, and ultimately complete regeneration of functional human tissues. Resilin is a super elastic and highly resilient natural protein with good biocompatibility but lacks specific biological and chemical cues. Therefore, resilin decorated with collagen I–binding domain is proposed as a functional nanocomposite template biomaterial. Collagen I is an ideal binding target, as it is the most abundant structural protein found in human body including scars that affect unwanted adhesion.

Future Work

Musculoskeletal-related injuries and disorders are the second largest cause of disabilities worldwide. Significant pain, neurological discomfort, limited mobility, and substantial financial burden are associated with these disorders. Thus, biocompatible materials comprised of resilin with collagen-binding domain, such as films adhesive bandages (films, fiber matts, or hydrogels), sutures, screws and rods, three-dimensional scaffolds, and delivery vehicles, will be designed and evaluated for multiple musculoskeletal-related regeneration applications.

Keywords Resilin · Collagen-binding domain · Stretchable nanocomposite · Functional biomaterials · Regenerative medicine

✉ Robert J. Linhardt
linhar@rpi.edu

[1] Center for Biotechnology and Interdisciplinary Studies, Rensselaer Polytechnic Institute, Troy, NY, USA

[2] Department of Chemistry and Chemical Biology, Rensselaer Polytechnic Institute, Troy, NY, USA

[3] Howard P. Isermann Department of Chemical and Biological Engineering, Rensselaer Polytechnic Institute, Troy, NY, USA

[4] Robert H. Smith Faculty of Agriculture, Food and Environment, Department of Plant Sciences and Genetics in Agriculture, The Hebrew University of Jerusalem, 76100 Rehovot, Israel

[5] The Center for Nanoscience and Nanotechnology, The Hebrew University of Jerusalem, 91904 Jerusalem, Israel

Introduction

Designing functional and multi-domain matrices and devices for the sensing, repair, and regeneration of tissues and organs remains a major challenge [1–3]. Engineered biomaterials need to withstand repetitive motion and environmental physical stresses common to dynamic tissues. To that end, elastomeric polymers are of great interest as functional materials due to their innate mechanical properties that closely mimic those of tissues [4, 5]. Indeed, a number of natural elastomeric polypeptides have been studied extensively for their potential use as biomaterials, including collagen, elastin, and recently resilin [4, 5]. Modular biopolymers with different biological domains, prepared using advanced recombinant technologies, have been engineered with protein-binding and cell-adhesive domains [6, 7].

Resilin is a rubber-like protein with extraordinary elasticity and resilience. It is found in the wing hinge ligament of locust (*Schistocerca gregaria*), the tendon of the pleuro-subtalar muscles in dragonflies (*Aeshna juncea*), and the sound-producing membrane, tymbal, in the cicada [8, 9]. Biological and physiological requirements have evolutionarily shaped resilin's diverse functionality. These required properties include stretching, shock absorbance or energy storage, vibrations up to 13 kHz, and as low as 0.6 MPa elastic modulus [5, 10–12]. The full-length resilin gene (CG15920) sequence was first identified in the *Drosophila melanogaster* genome and consists of three domains [13]. Exon I (the first exon), comprising 18 pentadecapeptide repeats (GGRPSDSYGAPGGGN), and exon III both encode the elastomeric sequences of resilin. Exon II has only 62 amino acids and is a cuticular chitin-binding domain [14, 15]. Most resilin-based structure-activity relationship (SAR) studies have relied on recombinant resilin-like polypeptide (RLP, also known as pro-resilin).

Resilin is an amorphous polymer composed of randomly coiled chains covalently connected through di- and tri-tyrosine cross-links, resulting in its isotropic behavior [5, 16]. Kaplan and colleagues [17] have studied the SAR of full-length resilin as well as smaller segments of resilin corresponding to exons I and III. The sequences of both exons I and III afford β-spirals made up of repeating β-turns with interspiral spacers that allow for a suspended-like chain configuration. The Fourier transform infrared (FTIR) spectroscopy and circular dichroism (CD) analysis from this study suggest that exons I and III, similar to full-length resilin, are amorphous random polymers. Furthermore, based on the AFM results, 93% and 86% of resilin resilience were attributable to exon I and exon III, respectively, when cross-linked. The higher flexibility of exon I was attributed to a greater number of hydrophilic amino acid sequences resulting in a more disordered structure.

A few studies have directly explored resilin for applications in regenerative medicine [18, 19]. Rivkin et al. [20] and Verker et al. [21] engineered resilin to include a cellulose-binding domain (CBD) and explored it potential to bind to cellulose nanocrystals (CNCs). Kiick and coworkers [20] have developed injectable resilin hydrogels for the repair and regeneration of vocal folds. These hydrogels were based on 12 repeats of the exon I–based pentadecapeptide RLP containing a variety of biologically active moieties, including a cell-binding (RGD) domain, a matrix metalloproteinase (MMP)–sensitive domain, and heparin-binding domain [20]. FTIR studies showed similar structurally disordered conformation for the cross-linked and soluble RLPs. Rheological studies revealed that hydrogels with different combinations of RLPs with biologically active moieties showed a similar storage modulus, indicating that the incorporation of biological domains had little effect on the mechanical properties of resilin. The same study also examined cell attachment, proliferation, and migration using human mesenchymal stem cells (hMSCs). RLP-RGD-based hydrogel films supported cell attachment and spreading and maintained the spindle-like morphology of these hMSCs. Encapsulated hMSCs in RLP-RGD alone or in combination with RLP-MMP polypeptide showed good biocompatibility but cell migration was limited to RLP-RGD hydrogels. Thus, optimal cellular growth, migration, and differentiation could be achieved by tuning the combination different biological domains within an RLP. Recently, the same group demonstrated the cytocompatibility of the injectable hydrogel in a mouse subcutaneous model for potential applications in regenerative medicine [21]. Although some early acute inflammation attributed to the cross-linker tris (hydroxymethyl phosphine) was observed, resilin showed good overall cytocompatibility.

The current study is motivated by the resilience and elasticity of resilin. An exon I–based RLP was designed to serve as an elastomeric template for regenerative devices, such as adhesive bandages or films, electrospun fibers, screws, sutures, and drug delivery vehicles. Resilin was engineered to include a collagen-binding domain (ColBD), as a tissue interface for bone, muscle, ligament, tendon, and skin. Exon I (Rec1) from the native resilin gene of *Drosophila* (CG15920), fused with ColBD (Res-ColBD) from ColH collagenase from *Clostridium histolyticum*, was cloned and expressed in *Komagataella pastoris* (formerly *Pichia pastoris*). The structural properties, of the resulting non-cross-linked resilin, were characterized by FTIR spectroscopy and the binding of Res-ColBD to collagen I was assessed qualitatively by SDS-PAGE. Atomic force microscopy (AFM) in force mode afforded force measurements that confirmed excellent binding of Res-ColBD to collagen I, thereby confirming the potential of this nanocomposite construct for regenerative medicine applications.

Materials and Methods

Design and Construction of Collagen-Binding Resilin Expression Vector

A synthetic collagen-binding resilin construct was designed by fusing resilin exon 1 [14, 15] with ColBD from ColH collagenase of *C. histolyticum* in place of resilin exon 2, the natural cuticular chitin-binding domain [22] (Fig. 1A). The codon sequences (CDS) for the synthetic Res-ColBD fusion protein were codon optimized for expression in *K. pastoris*. Insertion into the multiple cloning sites of vector pD912 (ATUM, Newark, CA) facilitated transcriptional control by the methanol inducible promoter AOX1 through integration into the AOX1 locus of the *K. pastoris* genome, and protein secretion was mediated by fusion to the N-terminal secretion signal tag from α-mating factor (Fig. 1B). Gene synthesis, cloning, genomic integration, and initial protein secretion screening steps were performed by ATUM.

Expression of the Recombinant Rec1-Res and Res-ColBD Protein

K. pastoris was patched on YPD (1% yeast extract, 2% peptone, 2% dextrose, 1.5% agar) plates with 250 μg/mL Zeocin and incubated for 3 days at 30 °C. Single colonies were inoculated into 2.5 mL of BMGY medium at pH 6 + 250 μg/mL Zeocin in 15-mL tubes. Tubes were shaken at 28 °C and 250 rpm for 48 h. Each tube was boosted thereafter twice/day with 25 μL of 1% (*v*/*v*) methanol and allowed to grow for 24 h to induce. Cultures were harvested 48-h post-induction. Cells were pelleted by spinning for 10 min at 1000×*g* at 4 °C. The expression and purification of exon I resilin (Rec1-Res, without ColBD) were previously described [15]. Rec1-Res was used in all assays as negative control.

ATR-FTIR

Attenuated total reflectance-Fourier transform infrared spectroscopy (ATR-FTIR) was used to analyze the characteristic differences of the structure of human collagen type I, Rec1-Res, and other proteins based on their IR absorption frequencies (Perkin Elmer Spectrum One FT-IR Spectrometer, USA). A few milligrams of freeze-dried protein sample were placed on the zinc selenide (ZnSe) crystal and the IR transmittance spectra were collected in the wave number range of 4000 to 650 cm^{-1} at a resolution of 4 cm^{-1}. All the spectra were normalized to eliminate the differences due to concentration and the thickness of the sample.

Binding of Res-ColBD to Collagen I

Qualitative binding potential of crude Res-ColBD was performed using lyophilized human type I collagen (Advanced BioMatrix, San Diego, CA). A total of 150 μg/mL of Res-ColBD was added to 150 μg of collagen I at neutral pH. Rec1-Res was used as a control to establish nonspecific interaction between resilin and collagen I. The mixture was incubated under gentle shaking for 30 min at room temperature. The mixture was centrifuged and the supernatant (unbound fraction) was removed, boiled with running buffer for 10 min, and analyzed using SDS-PAGE on a 4–20% gel.

AFM Imaging and Force Measurements

Collagen I sample was prepared by depositing 50 μL of collagen solution (3 mg/mL in acetic acid) onto a mica surface for 10-min adsorption. Non-adsorbed collagen I was washed away with deionized water. Three-dimensional images were collected in air using the AFM tapping mode technique and standard Si cantilevers (AC240TS, Olympus America, Center Valley, PA).

a

MRFPSIFTAVLFAASSALAAPVNTTTEDETAQIPAEAVIGYSD
LEGDFDVAVLPFSNSTNNGLLFINTTIASIAAKEEGVSLEKRE
AEAMGEPPVNSYLPPSDSYGAPGQSGPGGRPSDSYGAPGGGNG
GRPSDSYGAPGQGQGQGQGQGGYAGKPSDTYGAPGGGNGNGGR
PSSSYGAPGGGNGGRPSDTYGAPGGGNGGRPSDTYGAPGGGGN
GNGGRPSSSYGAPGQGQGNGNGGRSSSYGAPGGGNGGRPSDTY
GAPGGGNGGRPSDTYGAPGGGNNGRPSSSYGAPGGGNGGRPSD
TYGAPGGGNGNGSGGRPSSSYGAPGQGQGGFGGRPSDSYGAPG
QNQKPSDSYGAPGSGNGNGGRPSSSYGAPGSGPGGRPSDSYGP
PASGSGAGGAGGSGPGGADYDNDE**PVYPIGTEKEPNNSKETAS**
GPIVPGIPVSGTIENTSDQDYFYFDVITPGEVKIDINKLGYGG
ATWVVYDENNNAVSYATDDGQNLSGKFKADKPGRYYIHLYMFN
GSYMPYRINIEGSVGR

b

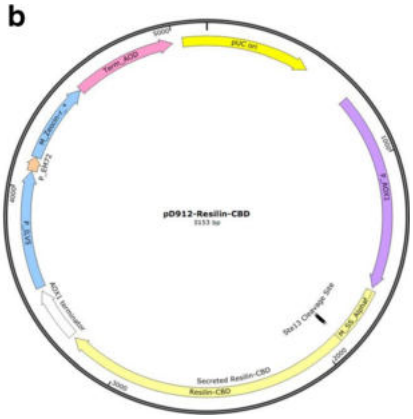

Fig.1 (A) Amino acid sequence of secreted collagen-binding resilin. Underline indicates cleaved α-mating factor secretion signal tag, and bold indicates collagen-binding domain. (B) Vector map for pD912-Resilin-ColBD

For the force measurements, Rec1-Res and Res-ColBD were covalently attached to AFM cantilevers, supplied with an immobilized 10-μm gold-coated borosilicate glass sphere (Novascan, Ames, IA), through a two-step protocol. In the first step, AFM probes were incubated with 2 mM HS-$(CH_2)_{11}$-PEG_6-COOH (Prochimia, Sopot, Poland) in ethanol, overnight and at RT; the sulfhydryl, the alkyl chain, the six polyethylene glycol (PEG) units, and the carboxyl group provide covalent attachment to gold, self-assembling, an inert layer, and the reactive group for protein coupling, respectively. In the second step, standard EDC/NHS chemistry was used to couple the protein to the modified AFM probes, carrying the –COOH groups using the following protocol: (i) rinse with phosphate buffer (PB) pH 6.0; (ii) incubate with 2 mM EDC and 5 mM NHS in PB pH 6.0 for 15 min at RT; (iii) rinse with PB pH 6.0; (iv) rinse with PBS pH 7.4; (v) incubate with ~ 0.2 mg/mL protein solutions in PBS pH 7.4, overnight at 4 °C; and (vi) rinse with PBS pH 7.4. Force spectroscopy scans were obtained in the force-volume mode [23, 24]. The AFM cantilevers were calibrated before each experiment, using a previously described three-step procedure [25]. Spring constants were within 10% error from the ones supplied by the manufacturer (i.e., 0.02 N/m). A force-volume data set consisted of an array of 400 (20 × 20) force measurements, scanning in contact mode at 2 μm/s an area of 20 × 20 μm^2, with each pixel point spanning an approximate width of 1 μm in both *X* and *Y*. The trigger force was set to 2 nN. All force measurements were performed using the MFP-3DTM atomic force microscope (Asylum Research, Santa Barbara, CA) and the collected data were analyzed using IGOR Pro 6 (WaveMetrics, Inc., Lake Oswego, OR).

Results

Res-ColBD plasmid was successfully constructed by fusing resilin exon 1 (Rec1) with collagen-binding domain (ColBD) from ColH collagenase of *C. histolyticum* (Fig. 1B). After transformation of the plasmid into *K. pastoris* (ATUM), expression was carried out and cells were induced with 1% methanol. Cultures were centrifuged 48-h post-induction and supernatant collected.

The conformational properties of Exon I (Rec1-Res) has been extensively studied. An FTIR spectrum of non-cross-linked Rec1-Res, Res-ColBD, and collagen I was obtained to confirm our results (Fig. 2). Based on the ATR-FTIR spectra, collagen I showed all expected characteristic peaks of human collagen type I. Rec1-Res and Res-ColBD were slightly different but showed similar IR absorption peaks [26]. The three proteins showed peaks corresponding to amide I (1700–1600 cm^{-1}), amide II (1480–1350 cm^{-1}), and amide III (1300–1230 cm^{-1}) stretching at approximately 1640, 1540, and 1240 cm^{-1}, respectively. All the protein spectra also

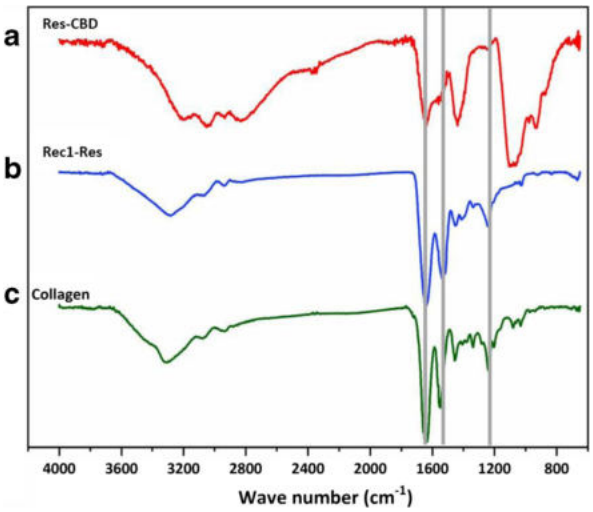

Fig. 2 ATR-FTIR spectra of lyophilized (A) Res-ColBD; (B) Rec1-Res; and (C) neat collagen I. Peaks corresponding to amide I (1700–1600 cm^{-1}), amide II (1480–1350 cm^{-1}), and amide III (1300–1230 cm^{-1}) are shown

appeared to contain amide A (3400–3100 cm^{-1}) and B (~2930 cm^{-1}) peaks that corresponds to hydroxyls and free amines of amide A group and alkyl stretching peaks of amide B group. Collagen I, Rec1-Res, and Res-ColBD exhibited IR absorptions at approximately 3300, 3300, and 3200 cm^{-1}, respectively, corresponding to NH groups involved in hydrogen bonding (νN-H). All three spectra also showed hydrogen bonded-hydroxyl bond stretching at around 3100 cm^{-1} [27]. The presence of hydrogen bonding in amide A group is indicative of the secondary structure of all three proteins. They also showed carbon-hydrogen alkyl bond stretching peaks (νC-H) at around 2950 to 2847 cm^{-1} and carbon-oxygen stretching peak (νC-O) at 1035 cm^{-1} [28]. Res-ColBD also showed a peak between 1100 and 800 cm^{-1} which corresponds to C–H bond and is possibly due to the ColBD presence in resilin nanocomposite. Similar peaks have been shown in other resilin fused with binding domains, such as cellulose-binding domain [29].

The ColBD was added to the elastomeric resilin to obtain added functionality allowing resilin nanocomposite to bind to collagen-containing tissues. Lyophilized collagen I incubated with water-soluble Res-ColBD or Rec1-Res at 1:1 ratio to examine collagen binding. After incubation for 30 min at room temperature, the mixture was centrifuged and unbound (supernatant) fractions were analyzed with SDS-PAGE (Fig. 3). Collagen I showed only two distinct bands, alpha (~ 120 kDA) and beta (~ 250 kDA). The gamma region was not observed due to its size, which is approximately 300 kDA; there was, however, a dark band inside the well suggested the presence of the gamma region. The Res-ColBD band was absent in the unbound fraction indicating complete binding to collagen I. The Rec1-Res band was observed in the

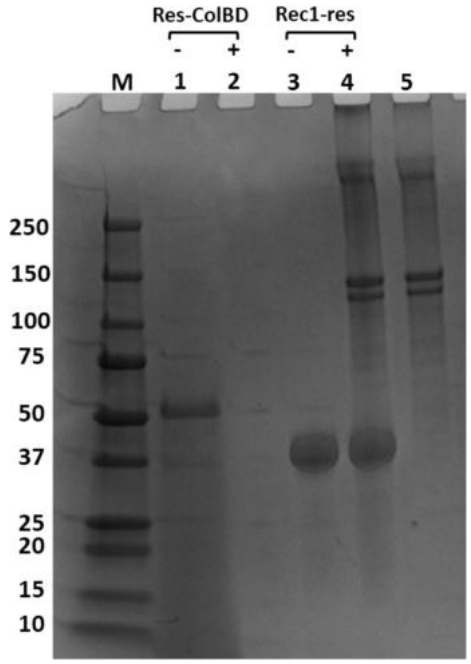

Fig. 3 Binding of Res-ColBD binding to collagen I. Res-ColBD, Rec1-Res, and insoluble collagen I were incubated in neutral pH for 30 min and analyzed by SDS-PAGE. Lane M, ladder; lane 1, Res-ColBD; lane 2, unbound fraction of Res-ColBD mixed with collagen I; lane 3, Rec1-Res; lane 4, unbound fraction of Rec1-Res mixed with collagen I; lane 5, collagen I. Numbers on the left are molecular masses (in kDa) of the ladder

unbound fraction along with collagen I bands indicating no binding of this construct was observed.

In addition to examining the specificity of this interaction, it was also important to determine the quantitative strength of interaction between Res-ColBD and collagen I. In the envisioned applications of a resilin capable of collagen binding, the strength of the resulting intermolecular forces between tissue and Res-ColBD needs to be sufficient to counteract the mechanical forces within the tissue being repaired. AFM was used to determine the binding strength of Res-ColBD with collagen at the molecular level to study this interaction. Collagen I was first physically absorbed as typical collagen fibrils onto a mica surface, allowed to dry, and images were taken (Fig. 4A). A spherical gold AFM tip on a cantilever was then used to probe the interaction between Res-ColBD or Rec1-Res (control) and the collagen surface. The spherical gold ASFM tip was first PEGylated (HS-$(CH_2)_{11}$-PEG_6-COOH) to minimize nonspecific interactions of the gold sphere with collagen-mica surface. The carboxyl groups on the PEG derivative were used for the attachment of either Res-ColBD or Rec1-Res (Fig. 4B). AFM force-distance curves were collected as the protein-functionalized tips approached the collagen-coated surface, were allowed to adhere, and then were retracted to measure the unbinding forces (Fig. 4C). Control experiments, with an unmodified gold AFM tip, were undertaken to measure the interaction with collagen I using adhesion forces ranging from 0.5 to 5 nN to determine the specificity of ColBD binding (Fig. 5). Histograms representing the frequency of the nonspecific adhesion force are shown in Fig. 5A and the corresponding adhesion force-volume maps are shown in Fig. 5B. Nonspecific interactions were minimized by the presence of the PEG layer and the residual nonspecific interactions (Fig. 6A, left) were excluded in the data analysis. In general, a single adhesion peak is observed in the Rec1-Res (control) force-distance plots (Fig. 6B), while multiple adhesion peaks were observed for Res-ColBD (Fig. 6C). Herman-Bausier and Dufrêne had previously demonstrated two distinct binding

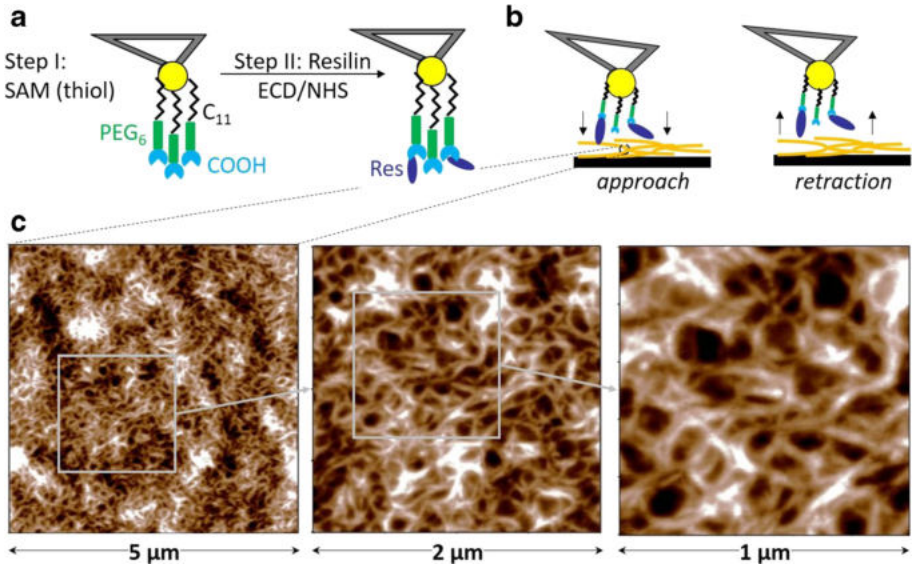

Fig. 4 Schematic representation of surface modifications. (A) PEGylation of AFM gold spear using self-assembled monolayer of (HS-$(CH_2)_{11}$-PEG6-COOH) (SAM) and conjugation of Res-ColBD or Rec1-Res using EDC/NHS modifications. (B) Approach and retraction of functionalized tip onto collagen-coated surface. (C) AFM images (5×5, 2×2, and 1×1 μm^2) of collagen I fibrils physically absorbed and dried onto the mica chip

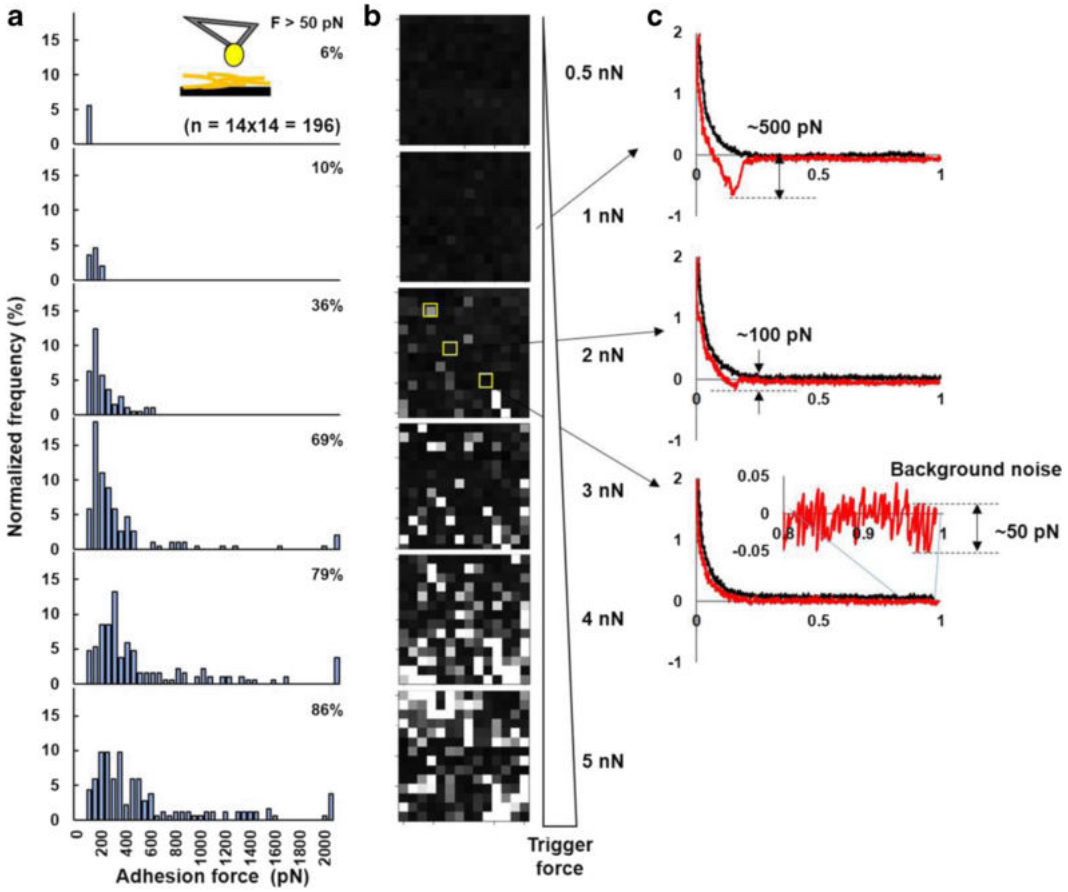

Fig. 5 Nonspecific interactions between unmodified gold tip and collagen by AFM spectroscopy using trigger forces ranging from 0.5 to 5 nN. (A) Histograms representing the frequency and distribution of adhesion forces above 50 pN (threshold), including the total frequency (%) versus the amount of measurements ($n = 196$). (B) Adhesion force-volume maps. (C) Example of three different force-distance curves. The trigger force (compression force during contact at short distances) was increased from top to bottom in (A) and (B)

events/peaks, a weak and a strong peak, are typically observed in ColBD and collagen interactions [30]. In the current study, a weak signature peak of 36 pN and a stronger signature peak of 91 pN were observed in the interaction of Res-ColBD with collagen I (Fig. 7A). In addition, above the major peaks in Res-ColBD, a few additional minor peaks were observed. Similar minor peaks have also been previously reported as associated with single-molecule interactions [31]. Interestingly, even at the single-molecule adhesion level, weak and strong peaks are observed. Thus, the primary signature

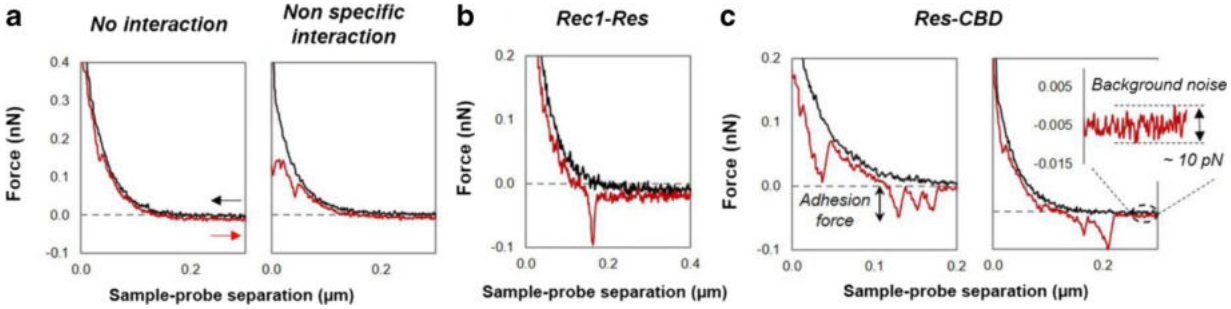

Fig. 6 Specific interactions between collagen and ColBD by AFM spectroscopy. (A) Example force-distance curves for (i) no interaction and (ii) nonspecific interaction. (B) Specific interactions of Rec1-Res with collagen I. (C) Specific interactions of Res-ColBD with collagen I, (left) a three-peak specific interaction curve; (right) a two-peak specific interaction curve. Arrows pointing up and down show compression and pullout, respectively

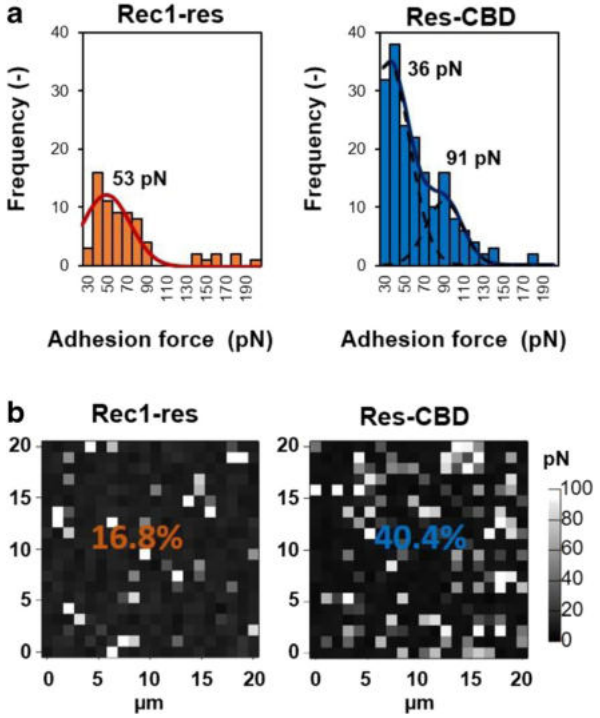

Fig. 7 Force mapping analysis of individual events by AFM. (A) The histograms represent the frequency of the adhesion force events above 20 pN for Rec1-Res (left) and Res-ColBD (right), fitted with a 1-peak and a 2-peak Gaussian curves, respectively. (B) Adhesion force-volume maps for Rec1-Res (left) and Res-ColBD (right) with collagen I. Nonspecific interactions are represented by dark pixels and specific interactions are represented by white pixels. The percentage of events with adhesion force above 20 pN is also reported. Each data set consisted of an array of 400 (20 × 20) force measurements, scanning in contact mode at 2 μm/s an area of 20 × 20 μm^2, with each pixel point spanning an approximate width of 1 μm in both *X* and *Y*. The trigger force was set to 2 nN

peaks for this interaction might also be the results of multiple, parallel binding events as shown in the Gaussian fitted curves (Fig. 7A). It is also noteworthy that the frequency of these events is significantly higher in the Res-ColBD than in the Rec1-Res. In the force maps of individual adhesion events, Rec1-Res shows a statically significantly lower frequency (16.7%) than does the frequency observed for the Res-ColBD (40.4%) (Fig. 7B).

Since both the frequency and strength of adhesion of the Res-ColBD nanocomposite are shown to be significantly higher, the mechanical stability needs to be addressed. Figure 8 illustrates the elastic properties, the stretching or unfolding of Res-ColBD nanocomposite. During AFM measurements, the Res-ColBD molecule, attached to AFM tip, adheres to collagen during contact and then becomes mechanically stretched as the tip is retracted away from collagen. The mechanical properties of Res-ColBD are then recorded in the form of force-distance (FD) curves and analyzed using the worm-like chain (WLC) model of polymer [32].

$$F(x) = \frac{k_B T}{L_p}\left[\frac{1}{4}\left(1-\frac{x}{L_C}\right)^{-2} - \frac{1}{4} + \frac{x}{L_C}\right]$$

where $F(x)$ is the distance-dependent force (kg m s^{-2}), x is the extension length (m), k_B is Boltzmann's constant, T is the temperature (K), L_p is the persistence length (m), and L_C is the contour length (m) of the chain. L_p measures the stiffness (i.e., bending and rigidity) of the chain molecule and is an intrinsic property of the material. L_C represents the theoretical length of stretched molecule. Since extension length (x) of each force curve varies, this is normalized by the fitted contour length (x/L_C). The data in Fig. 8B show that the average L_p is 4.65 nm which is longer than the peptide backbone length of a single amino acid residue [33]. The results indicate that Res-ColBD molecule exhibits a flexibility of a folded polypeptide chain even after 400 force measurements. Closer examination of the table in Fig. 8B, peak curve (18, 12) has the lowest L_p value of 1.29 nm which when corresponds to the WLC fitting of a single peak in Fig. 8C. This value is still significantly higher than length of a single amino acid residue, while peaks (17, 7 a, b and c) show even higher L_p values, which is indicative of multiple parallel binding events. Taken together with normalized stretching length of at least 90% (x/L_C) concludes that flexibility of Res-ColBD is not affected by its anchoring to collagen molecules.

Discussion

There is a clear need to develop new mechanically and biologically functional biomaterials for regenerative engineering applications. Among the many requirements for 3D scaffolds or devices for the repair and regeneration of tissues are the biocompatibility, degradation rate, architecture, and surface chemistry; however, often, the absence of adequate mechanical properties becomes a limiting factor [34, 35]. Tissues and organs are under constant internal and external mechanical loading; thus, designing biomaterials, which can accommodate these forces while maintaining integrity, becomes very challenging. Nature has rewarded us with a plethora of proteins and polypeptides having diverse biological and mechanical properties based on their various intended functionalities across many different species. These polypeptides have reached near evolutionary perfection over billions of years. One such example is the super elastic resilin, a cuticular protein found in specialized regions of many arthropods where repetitive motion, stretching, and jumping are required such as the wings of *Drosophila melanogaster*, the tendon of the pleuro-subtalar muscles in dragonflies, and the sound-producing membrane in the cicada.

The resilin gene (CG15920) from *D. melanogaster* consists of three distinct regions: an N-terminal region composed of 18

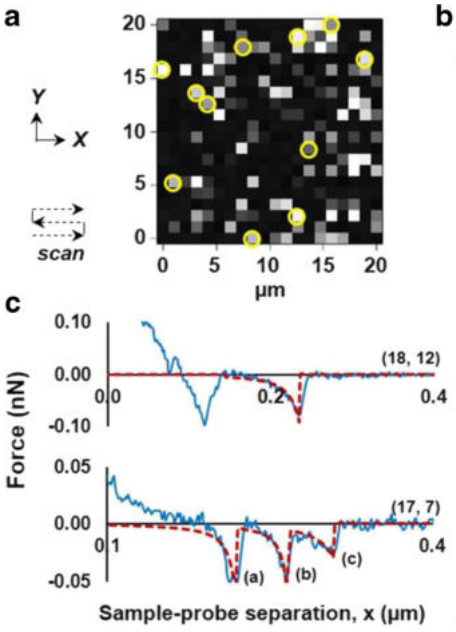

b

(X, Y)	L_p (nm)	x/L_C (-)
0, 8	3.25	0.937
2, 12	3.24	0.945
5, 1	2.58	0.929
8, 13	5.27	0.924
12, 4	2.62	0.918
13, 3	5.81	0.955
15, 0 (a)	5.94	0.944
15, 0 (b)	4.31	0.936
16, 18	6.03	0.951
17, 7 (a)	5.77	0.945
17, 7 (b)	12.71	0.959
17, 7 (c)	4.02	0.906
18, 12	1.29	0.905
19, 15	2.33	0.911

Fig. 8 Resilin stability during force mapping. (A) Adhesion force-volume map for Res-CBD as in Fig. 7B. The (*x*, *y*) coordinates have been introduced to better identify the individual force curves, and the time scan direction is also indicated. Yellow circles show the adhesion peaks that have been fitted using the WLC model. (B) Table summarizing the results from the WLC model fitting. (C) Examples of WLC fitting, for the case of a single peak as in (18, 12) scan, as well as three peaks in (17, 7) scan

copies of GGRPSDSYGAPGGGN motif (exon I), a chitin-binding domain (exon II, ChBD), and a C-terminal region composed of 11 copies of GYSGGRPGGQDLG motif (exon III) [17]. The elastic and resilient properties of resilin are attributed to the highly repetitive elastic segments of exons I and III. These segments are randomly coiled and linked together through the oxidation of tyrosine residues to form di- and tri-tyrosine links. Both exons I and III assemble into many well-defined β-turns structures, which then form β-spirals. Although the self-assembly of resilin into β-spirals is not unique in naturally occurring polypeptides, the work by Andrell et al. suggested that these β-spirals might be larger and more irregular than other elastomers, thereby giving resilin its exceptional mechanical properties [5]. The high fraction of hydrophilic residues, particularly in exon I, may be critical in the underlining sliding mechanism for resilin's greater elastic behavior as these minimize hydrophobic interactions.

Many studies have focused on understanding the SAR of full-length resilin or of exon I and exon III. The chitin-binding domain (ChBD) (exon II) suggests a role in anchoring resilin to chitin-rich surrounding tissue in the insect. Qin and co-workers demonstrated that exon II was in fact a chitin-binding domain with a high affinity towards cuticle chitin [14]. Resilin functional properties are based on the combination of the super elastic properties of exons I and III, with the adhesive nature of the ChBD in exon II, responsible for binding to the surrounding insect exoskeleton. Based on this logic, we examined naturally occurring resilin (exons I and III) as a highly elastic template, into which a ColBD was introduced, to design a functional binding polypeptide-based nanocomposite biomaterial. We were motivated by the need for a mechanically superior biomaterial with good biocompatibility and cytocompatibility that could withstand the repetitive load exerted on tissues while maintaining its integrity for prolonged periods of time. Collagen I is the most abundant extracellular structural protein in many tissues of the human body as well scar tissues. Therefore, a resilin decorated with collagen-binding domain could serve as a biomaterial for use in films, adhesive bandages [36, 37] (films, fiber matts, or hydrogels), sutures, screws and rods, 3D scaffolds, and delivery vehicles. Thus, the ChBD was replaced with collagen I–binding domain to ensure seamless healing and good adhesion to the surrounding human tissue.

Musculoskeletal-related injuries and disorders are the second largest cause of disabilities worldwide. Significant pain, neurological discomfort, limited mobility, and substantial financial burden are associated with these disorders [36–39]. Intervertebral disc (IVD), lower extremities, and knee-related disorders or injuries are common musculoskeletal procedures. Treatment usually requires invasive surgical procedures and prolonged pain management and follow-up procedures are common. Thus, patient quality of life is adversely impacted resulting in a significant socioeconomic burden.

Tissue engineering strategies have been developed in recent years to alleviate the burden of currently available treatment by fully restoring the structure and function of damaged tissue [40, 41]. Examples of such strategies include polymeric sutures, meshes, or plugs for intervertebral disc (IVD)–related disorders [42]. The IVD is comprised of three regions, a gelatinous core called the nucleus pulposus (NP), a fibrocartilaginous anulus fibrosus

(AF) envelop, and cartilaginous end plates on surrounding bony structures [43]. Damage or tearing in the AF layer causes disc herniation (slipping of NP core) impinging on the peripheral nerves. AF is composed of collagen fibers, mainly collagen I, and its main function is to resist the high tensile stresses caused by flexion-extension, bending, and pressurized NP core. These tissue engineering devices are typically made of metals, such as titanium, or polymers such as alginate, collagen, chitosan, silk, polylactic acid (PLA), poly(glycolic) acid, and poly(lactic-co-glycolic) acid (PLGA) [41, 42]. Although these polymers are good candidates, none match the elastic and resilient strength of resilin. Such elastic strength is required for the repetitive load-bearing tissues such as IVD and bones [44]. Although synthetic PLA, PGA, and PLGA can be chemically modified or blended with other biomaterials in an effort to increase their elasticity, they remain relatively stiff and can further damage the surrounding tissue [45, 46]. The use of metals as an alternative material can also cause further damage because their mechanical properties are much higher than bone. More importantly, the biomaterial-tissue interface becomes a critical aspect of the design [47]. Most such materials, although biocompatible, adhere only very weakly to surrounding tissues. Further chemical modification or the addition of biological moieties is often required. Therefore, by engineering a nanocomposite of resilin and collagen-binding domain might address the limitations of current tissue engineering strategies.

Previous studies have shown that exon I is more resilient than exon III. Indeed, combining exon III with exon I did not significantly improve the overall elasticity and resilience of resilin [15]. Therefore, we examined the potential use of a polypeptide encoded by exon I that had been functionalized with collagen-binding domain as the template biomaterial for multiple regenerative devices such as adhesive bandages or films, electrospun fibers, screws, sutures, and drug delivery vehicles. Exon I (Rec1) from the native resilin gene of *Drosophila* (CG15920) fused with collagen-binding domain (ColBD) from ColH collagenase of *C. histolyticum* was successfully cloned and expressed in methylotrophic *K. pastoris* (Fig. 1B). Although Res-ColBD was not tagged, since the protein was expressed in the culture supernatant, its purification was easily performed by centrifugation. Indeed, some of the other major advantages of using *K. pastoris* as an expression host includes its ability to be grown in very high cell densities, producing gram-scale amounts of products [48]. AXO1, a tightly regulated promoter, was used with in pD912 vector to promote the overexpression of proteins in simple and relatively inexpensive media. FTIR analysis of both Res-ColBD and Rec1-Res shows all the same major character peaks characteristic of Rec1-Res with minor differences in Res-ColBD having bands at 1200–800 cm^{-1} possibly due to the presence of a collagen-binding domain.

Many collagen-binding domains having different morphologies and biological roles exist in nature. Mammalian ColBD proteins, such as MMPs, engage in the remodeling of tissues, and thus, their prolonged presence may cause unfavorable outcomes [49]. A goal here is to anchor the resilin protein to damaged tissues to allow repair and regeneration. Bacterial ColBDs have generally evolved specifically to target mammalian collagen and ensure tight binding to the tissue [22]. Bacterial ColBDs are much smaller than their mammalian counterparts, which is advantageous when expressing a ColBD in a fusion protein. Gel electrophoresis analysis showed Res-ColBD bound very tightly to collagen I with no band present in the unbound fraction. When mixed with collagen, Rec1-Res band was present in the unbound fraction demonstrating limited, if any, nonspecific interactions. AFM studies were carried out to examine the binding specificity as well as to confirm the strength of the interaction between ColBD and collagen I.

Although a single-peak in Rec1-Res was observed (Fig. 6B), nonspecific interactions are possible due to two different possible nonspecific events: (i) the binding of unmasked COOH groups, as a result of PEGylating ($HS\text{-}(CH_2)_{11}\text{-}PEG_6\text{-}COOH$) the spherical tip with collagen I, and (ii) indentation caused by the high force (2 nN) can result in nonspecific tip-collagen interactions [50]. The frequency of these nonspecific interactions is significantly lower for the Rec1-Res-collagen interaction. Res-ColBD interaction with collagen resulted in two Gaussian curves/peaks, typical of a ColBD binding profile [31]. Multiple binding events are possible because of the nature of the AFM probe, its chemical modification, and its spherical shape. Thus, multiple (i.e., 2, 3, or more) resilin molecules might bind at the same time to collagen and result in different binding/unbinding peaks. This explains the presence of a third major peak for Res-ColBD, which seems to be of similar magnitude to one of the other peaks. Moreover, based on the adhesion force-volume map, Res-ColBD is statistically significantly higher than unfunctionalized Rec1 resilin.

The resilience of native resilin stems from its random coils made up of secondary β-spirals configuration with inter-spiral spacers which in turn allow for a suspended-like chain [17]. Thus, we examined whether Res-ColBD maintained its folded configuration when tethered and released repetitively. The present AFM study shows no conformational changes occurred to Res-ColBD during repetitive force stretching even at 90% extension. These results unequivocally demonstrate the intrinsic elasticity and resilience of Res-ColBD nanocomposite.

Conclusion

A collagen I–binding domain from ColH collagenase of *C. histolyticum* was successfully fused to exon I resilin (Res-ColBD) and the recombinant plasmid was expressed in *K. pastoris*. The engineered Res-ColBD nanocomposite was compared with non-functionalized exon I–based protein (Rec1-Res). SDS-PAGE data showed 100% binding of Resilin-ColBD (Res-ColBD) to collagen I, while Rec1-Res showed no binding. AFM intermolecular force results show a bimodal binding profile, which is typical of a ColBD-binding interaction. Moreover, based on the adhesion force-volume map, Res-ColBD was statistically significantly higher than resilin without ColBD. Thus, the resilin polypeptide-based nanocomposite biomaterial design presented here demonstrates the unique opportunity to engineer multi-domain biopolymer with different functionalities. This modular design not only can be used to target a specific tissue but also can be further functionalized by the addition of growth factors and/or cells to enhance its regenerative potential.

Funding Information This work was supported by the funding from the National Institutes of Health grant no. AR064157 Supplement to RJL. The AFM force measurements were supported by a US DOE grant (DOE Grant No. DE-FG02-09ER16005) to GB.

References

1. Jin H-E, Jang J, Chung J, Lee HJ, Wang E, Lee S-W, et al. Biomimetic self-templated hierarchical structures of collagen-like peptide amphiphiles. Nano Lett. 2015;15:7138–45. https://doi.org/10.1021/acs.nanolett.5b03313.
2. Woolfson DN, Mahmoud ZN. More than just bare scaffolds: towards multi-component and decorated fibrous biomaterials. Chem Soc Rev. 2010;39:3464–79. https://doi.org/10.1039/c0cs00032a.
3. Chen F-M, Liu X. Advancing biomaterials of human origin for tissue engineering. Prog Polym Sci. 2016;53:86–168. https://doi.org/10.1016/j.progpolymsci.2015.02.004.
4. Sutherland TD, Rapson TD, Huson MG, Church JS, Recombinant structural proteins and their use in future materials, in: Springer, Cham, 2017: pp. 491–526. https://doi.org/10.1007/978-3-319-49674-0_15.
5. Li L, Charati MB, Kiick KL. Elastomeric polypeptide-based biomaterials. Polym Chem. 2010;1:1160–70. https://doi.org/10.1039/b9py00346k.
6. DiMarco RL, Heilshorn SC. Multifunctional materials through modular protein engineering. Adv Mater. 2012;24:3923–40. https://doi.org/10.1002/adma.201200051.
7. Girotti A, Orbanic D, Ibáñez-Fonseca A, Gonzalez-Obeso C, Rodríguez-Cabello JC. Recombinant technology in the development of materials and systems for soft-tissue repair. Adv Healthc Mater. 2015;4:2423–55. https://doi.org/10.1002/adhm.201500152.
8. Andersen SO. Studies on resilin-like gene products in insects. Insect Biochem Mol Biol. 2010;40:541–51. https://doi.org/10.1016/j.ibmb.2010.05.002.
9. Charati MB, Ifkovits JL, Burdick JA, Linhardt JG, Kiick KL. Hydrophilic elastomeric biomaterials based on resilin-like polypeptides. Soft Matter. 2009;5:3412–6. https://doi.org/10.1039/b910980c.
10. Li L, Kiick KL. Resilin-based materials for biomedical applications. ACS Macro Lett. 2013;2:635–40. https://doi.org/10.1021/mz4002194.
11. Michels J, Appel E, Gorb SN. Functional diversity of resilin in Arthropoda. Beilstein J Nanotechnol. 2016;7:1241–59. https://doi.org/10.3762/bjnano.7.115.
12. Elvin CM, Carr AG, Huson MG, Maxwell JM, Pearson RD, Vuocolo T, et al. Synthesis and properties of crosslinked recombinant pro-resilin. Nature. 2005;437:999–1002. https://doi.org/10.1038/nature04085.
13. Ardell DH, Andersen SO. Tentative identification of a resilin gene in Drosophila melanogaster. Insect Biochem Mol Biol. 2001;31:965–70. https://doi.org/10.1016/S0965-1748(01)00044-3.
14. Qin G, Lapidot S, Numata K, Hu X, Meirovitch S, Dekel M, et al. Expression, cross-linking, and characterization of recombinant chitin binding resilin. Biomacromolecules. 2009;10:3227–34. https://doi.org/10.1021/bm900735g.
15. Qin G, Rivkin A, Lapidot S, Hu X, Preis I, Arinus SB, et al. Recombinant exon-encoded resilins for elastomeric biomaterials. Biomaterials. 2011;32:9231–43. https://doi.org/10.1016/j.biomaterials.2011.06.010.
16. Li L, Teller S, Clifton RJ, Jia X, Kiick KL. Tunable mechanical stability and deformation response of a resilin-based elastomer. Biomacromolecules. 2011;12:2302–10. https://doi.org/10.1021/bm200373p.
17. Qin G, Hu X, Cebe P, Kaplan DL. Mechanism of resilin elasticity. Nat Commun. 2012;3:1003. https://doi.org/10.1038/ncomms2004.
18. McGann CL, Levenson EA, Kiick KL. Resilin-based hybrid hydrogels for cardiovascular tissue engineering. Macromolecules. 2013;214:203–13. https://doi.org/10.1002/macp.201200412.
19. Li L, Mahara A, Tong Z, Levenson EA, McGann CL, Jia X, et al. Recombinant resilin-based bioelastomers for regenerative medicine applications. Adv Healthc Mater. 2016;5:266–75. https://doi.org/10.1002/adhm.201500411.
20. Li L, Tong Z, Jia X, Kiick KL. Resilin-like polypeptide hydrogels engineered for versatile biological function. Soft Matter. 2013;9:665–73. https://doi.org/10.1039/C2SM26812D.
21. Li L, Stiadle JM, Levendoski EE, Lau HK, Thibeault SL, Kiick KL. Biocompatibility of injectable resilin-based hydrogels. J Biomed Mater Res A. 2018;106:2229–42. https://doi.org/10.1002/jbm.a.36418.
22. Wilson JJ, Matsushita O, Okabe A, Sakon J. A bacterial collagen-binding domain with novel calcium-binding motif controls domain orientation. EMBO J. 2003;22:1743–52. https://doi.org/10.1093/emboj/cdg172.
23. A-Hassan E, Heinz WF, Antonik MD, D'Costa NP, Nageswaran S, Schoenenberger C-A, et al. Relative microelastic mapping of living cells by atomic force microscopy. Biophys J. 1998;74:1564–78. https://doi.org/10.1016/S0006-3495(98)77868-3.
24. Rotsch C, Braet F, Wisse E, Radmacher M. AFM imaging and elasticity measurements on living rat liver macrophages. Cell Biol Int. 1997;21:685–96. https://doi.org/10.1006/cbir.1997.0213.
25. Sorci M, Dassa B, Liu H, Anand G, Dutta AK, Pietrokovski S, et al. Oriented covalent immobilization of antibodies for measurement of intermolecular binding forces between zipper-like contact surfaces of split inteins. Anal Chem. 2013;85:6080–8. https://doi.org/10.1021/ac400949t.
26. Belbachir K, Noreen R, Gouspillou G, Petibois C. Collagen types analysis and differentiation by FTIR spectroscopy. Anal Bioanal Chem. 2009;395:829–37. https://doi.org/10.1007/s00216-009-3019-y.

27. Júnior ZSS, Botta SB, Ana PA, França CM, Fernandes KPS, Mesquita-Ferrari RA, et al. Effect of papain-based gel on type I collagen - spectroscopy applied for microstructural analysis. Sci Rep. 2015;5:11448. https://doi.org/10.1038/srep11448.
28. Rizk MA, Mostafa NY. Extraction and characterization of collagen from buffalo skin for biomedical applications. Orient J Chem. 2016;32:1601–9. https://doi.org/10.13005/ojc/320336.
29. Rivkin A, Abitbol T, Nevo Y, Verker R, Lapidot S, Komarov A, et al. Bionanocomposite films from resilin-CBD bound to cellulose nanocrystals. Ind Biotechnol. 2015;11:44–58.
30. Herman-Bausier P, Dufrêne YF. Atomic force microscopy reveals a dual collagen-binding activity for the staphylococcal surface protein SdrF. Mol Microbiol. 2016;99:611–21. https://doi.org/10.1111/mmi.13254.
31. Huang X, Li X, Wang Q, Dai J, Hou J, Chen L. Single-molecule level binding force between collagen and collagen binding domain-growth factor conjugates. Biomaterials. 2013;34:6139–46. https://doi.org/10.1016/J.BIOMATERIALS.2013.04.057.
32. Bustamante C, Marko JF, Siggia ED, Smith S. Entropic elasticity of λ-phage DNA. Science. 1994;265:1599–600.
33. Lim RYH, Köser J, Huang N, Schwarz-Herion K, Aebi U. Nanomechanical interactions of phenylalanine–glycine nucleoporins studied by single molecule force–volume spectroscopy. J Struct Biol. 2007;159:277–89.
34. O'Brien FJ. Biomaterials & scaffolds for tissue engineering. Mater Today. 2011;14:88–95. https://doi.org/10.1016/S1369-7021(11)70058-X.
35. Dhandayuthapani B, Yoshida Y, Maekawa T, Kumar DS. Polymeric scaffolds in tissue engineering application: a review. Int J Polym Sci. 2011;2011:1–19. https://doi.org/10.1155/2011/290602.
36. Brennan-Olsen SL, Cook S, Leech MT, Bowe SJ, Kowal P, Naidoo N, et al. Prevalence of arthritis according to age, sex and socioeconomic status in six low and middle income countries: analysis of data from the World Health Organization study on global AGEing and adult health (SAGE) Wave 1. BMC Musculoskelet Disord. 2017;18:271. https://doi.org/10.1186/s12891-017-1624-z.
37. Briggs AM, Cross MJ, Hoy DG, Sànchez-Riera L, Blyth FM, Woolf AD, et al. Musculoskeletal health conditions represent a global threat to healthy aging: a report for the 2015 World Health Organization World Report on Ageing and Health. Gerontologist. 2016;56:S243–55. https://doi.org/10.1093/geront/gnw002.
38. Dowdell J, Erwin M, Choma T, Vaccaro A, Iatridis J, Cho SK. Intervertebral disk degeneration and repair. Neurosurgery. 2017;80:S46–54. https://doi.org/10.1093/neuros/nyw078.
39. K.R. Fingar, C. Stocks, A.J. Weiss, C.A. Steiner, Most frequent operating room procedures performed in U.S. hospitals, 2003-2012 #186, (n.d.). https://www.hcup-us.ahrq.gov/reports/statbriefs/sb186-Operating-Room-Procedures-United-States-2012.jsp.
40. Langer R, Vacanti JP. Tissue engineering. Science. 1993;260:920–6 http://www.ncbi.nlm.nih.gov/pubmed/8493529 (accessed October 29, 2018).
41. Yu X, Tang X, Gohil SV, Laurencin CT. Biomaterials for bone regenerative engineering. Adv Healthc Mater. 2015;4:1268–85. https://doi.org/10.1002/adhm.201400760.
42. Sebastine IM, Williams DJ. Current developments in tissue engineering of nucleus pulposus for the treatment of intervertebral disc degeneration. Conf Proc Annu Int Conf IEEE Eng Med Biol Soc IEEE Eng Med Biol Soc Annu Conf. 2007;2007:6401–6. https://doi.org/10.1109/IEMBS.2007.4353821.
43. Richardson SM, Mobasheri A, Freemont AJ, Hoyland JA. Intervertebral disc biology, degeneration and novel tissue engineering and regenerative medicine therapies. Histol Histopathol. 2007;22:1033–41. https://doi.org/10.14670/HH-22.1033.
44. Hudson KD, Alimi M, Grunert P, Härtl R, Bonassar LJ. Recent advances in biological therapies for disc degeneration: tissue engineering of the annulus fibrosus, nucleus pulposus and whole intervertebral discs. Curr Opin Biotechnol. 2013;24:872–9. https://doi.org/10.1016/J.COPBIO.2013.04.012.
45. Washington MA, Balmert SC, Fedorchak MV, Little SR, Watkins SC, Meyer TY. Monomer sequence in PLGA microparticles: effects on acidic microclimates and in vivo inflammatory response. Acta Biomater. 2018;65:259–71. https://doi.org/10.1016/J.ACTBIO.2017.10.043.
46. Agrawal CM, Athanasiou KA, Technique to control pH in vicinity of biodegrading PLA-PGA implants, John Wiley & Sons, 1997. https://doi.org/10.1002/(SICI)1097-4636(199722)38:2<105::AID-JBM4>3.0.CO;2-U.
47. Iatridis JC, Nicoll SB, Michalek AJ, Walter BA, Gupta MS. Role of biomechanics in intervertebral disc degeneration and regenerative therapies: what needs repairing in the disc and what are promising biomaterials for its repair? Spine J. 2013;13:243–62. https://doi.org/10.1016/J.SPINEE.2012.12.002.
48. Ahmad M, Hirz M, Pichler H, Schwab H. Protein expression in Pichia pastoris: recent achievements and perspectives for heterologous protein production. Appl Microbiol Biotechnol. 2014;98(12):5301–17. https://doi.org/10.1007/s00253-014-5732-5.
49. Leitinger B, Hohenester E. Mammalian collagen receptors. Matrix Biol. 2007;26:146–55. https://doi.org/10.1016/J.MATBIO.2006.10.007.
50. Lamontagne C-A, Grandbois M. PKC-induced stiffening of hyaluronan/CD44 linkage; local force measurements on glioma cells. Exp Cell Res. 2008;314:227–36.